Underwater synthetic image generation for multi-temporal monitoring of crustose coralline algae

Alessio Calantropio [1], Alessia Giaquinto [1], Silvio Del Pizzo [1], Fabio Menna [2], Erica Nocerino [3]

[1] Department of Science and Technology, University of Napoli Parthenope, Napoli, Italy – alessio@calantropio.it; alessia.giaquinto001@studenti.uniparthenope.it; silvio.delpizzo@uniparthenope.it
[2] Department of Chemical, Physical, Mathematical and Natural Sciences, University of Sassari, Sassari, Italy – fmenna@uniss.it
[3] Department of Humanities and Social Sciences, University of Sassari, Sassari, Italy - enocerino@uniss.it

Keywords: Underwater photogrammetry, Neural Radiance Field (NeRF), Synthetic image generation, multi-temporal monitoring, Radiometric correction, Ecological conservation.

Abstract

Monitoring crustose coralline algae (CCA) is crucial for understanding the health and evolution of marine ecosystems. In particular, CCA-dominated assemblages serve as key indicators of ecological change, especially in the context of global climate pressures and ocean acidification. Developing robust tools to detect subtle and spatially distributed variations in their appearance is fundamental for early warning systems and practical conservation actions. However, acquiring multitemporal underwater images with reliable ground truth is complex due to environmental variability and logistical challenges. This paper proposes a framework integrating underwater photogrammetry with Neural Radiance Fields (NeRF) to create synthetic images for multi-temporal ecological monitoring. The authors investigate the creation of synthetic views from consistent camera positions across various monitoring periods to enhance the consistency and interpretability of image-based evaluations over time. More specifically, we have focused on generating synthesized images with the same camera pose across different epochs to assess expected environmental changes, enabling repeatable, ground-truth-validated tests of image-based monitoring techniques. A quantitative image comparison framework was developed, incorporating several metrics, such as Peak Signal-to-Noise Ratio (PSNR), Structural Similarity Index Measure (SSIM), and perceptual color difference (ΔE) within spatially constrained masks in specific regions of interest (ROIs). Results demonstrate the ability to detect chromatic alterations over time, with SSIM values indicating consistency and ΔE metrics revealing widespread perceptual changes. The methodology provides a robust and reproducible foundation for evaluating monitoring protocols and supporting ecological interpretation.

1. Introduction

Marine ecosystems are constantly affected by climate change and human activities, requiring rigorous ecological monitoring to assess their health, evolution, and the effectiveness of the protection measures implemented. The MANATEE (Monitoring and mApping of mariNe hAbitat with inTegrated gEomatics technologiEs) project (Nocerino et al., 2023) is developing advanced geomatic techniques for performing surveys in the underwater environment, as well as defining multi-temporal monitoring protocols. These protocols will allow scientists to collect metric data on sub-centimetre changes in benthic communities exposed to environmental stresses. Understanding the impact of environmental changes on marine habitats requires innovative monitoring solutions. Within the MANATEE project, this research explores the integration of photogrammetry and Neural Radiance Fields (NeRFs) for generating synthesized images (Mildenhall et al., 2020), thereby improving the multi-temporal analysis of *Lithophyllum stictiforme* (*L. stictiforme*), a crustose coralline alga (CCA) that is a fundamental bioconstruction of coralligenous reefs in the Mediterranean Sea (Pinna et al., 2022).

This study assesses the inspection methods of domain experts, such as archaeologists and ecologists, who primarily rely on 2D data comparison rather than 3D data over time. This approach could be beneficial for detecting phenomena like bleaching caused by environmental stressors, including rising temperatures and pollution. This is particularly relevant for ecological studies, where acquisition conditions may vary for environmental or logistical reasons. By rendering synthetic views from consistent camera poses across different epochs, comparing the same portion of the reef becomes possible under standardized viewing conditions. As a result, the rendered views serve as a powerful tool to support repeatable, accurate, and interpretable multi-temporal analysis, especially in ecological contexts where physical access and imaging conditions can vary significantly between surveys.

1.1 The rise of Neural Radiance Fields and its complementarity with traditional photogrammetry

For a long time, 3D modelling techniques have proven effective in various application fields. Among these, photogrammetry stands out for its versatility and usefulness in different contexts. In recent years, traditional photogrammetry has been complemented by computer vision-based approaches, namely structure from motion (SfM) and multi-view stereo (MVS). SfM is a computer vision method that reconstructs a 3D representation of a scene from 2D images, leveraging the principle of parallax by analyzing how distinctive points of an object or scene move across images captured from different angles or positions. Conversely, MVS algorithms focus on creating a detailed 3D representation of a scene using numerous images from various viewpoints. Unlike SfM, which primarily emphasizes reconstructing the global geometry of the scene and camera positions, MVS prioritizes enhancing the point cloud to achieve a more detailed 3D reconstruction.

Recently, the field has been transformed by the rise of artificial intelligence (AI)- based methods, particularly deep neural networks. Notably, NeRFs signify a significant advancement over traditional methods. Introduced by Mildenhall et al. (Mildenhall et al., 2020, 2019), NeRF is a groundbreaking technique for view synthesis using neural networks. This approach outlines a method for representing and reconstructing

3D scenes using 2D images captured from diverse angles. The essence of this technique lies in employing a deep neural network to learn a continuous function that links each point in 3D space, along with a view direction, to two variables: the color (RGB) for that particular direction and the volumetric density, which indicates the opacity or the capacity of the point to emit or reflect light.

NeRF uses a differentiable volumetric rendering algorithm that mimics the light's path through the scene, fine-tuning the model's parameters based on the provided images to produce new views of a scene. These images must showcase different perspectives of the scene and necessitate accurate knowledge of the positions and orientations of the capturing cameras. One of NeRF's key advantages is its ability to create photorealistic synthesized views with impressive detail, surpassing traditional methods that rely on voxel or mesh representations (Mildenhall et al., 2020). However, NeRF also has certain limitations: it requires a substantial number of input images and precise camera position data. It is computationally demanding, which poses challenges for real-time rendering.

In recent years, comparisons between 3D reconstruction using photogrammetry and those achieved with AI, particularly NeRF, have drawn significant attention from the scientific community, as Researchers seek to assess the practicality and effectiveness of applying the innovative NeRF methodology in photogrammetry (Croce et al., 2024; (Pepe et al., 2023)). Focusing on the step just before rendering new scenes makes it feasible to extract the point cloud generated by NeRF for research purposes.. The findings indicate NeRF techniques surpass traditional photogrammetry when reconstructing objects with challenging surfaces, such as textureless or reflective properties. However, photogrammetry is more effective for objects with well-defined textures. The authors propose that these methods are complementary, and their combined use could improve future 3D reconstruction applications (Remondino et al., 2023).

Despite the promising potential of NeRF-based reconstruction, higher deviations observed in the C2M analysis, particularly the higher standard deviations in NeRF outputs, highlight certain limitations. These discrepancies may stem from factors such as the sparse input sampling, view-dependent radiance effects, or the inherent smoothing behavior of volumetric rendering techniques, which can blur fine geometric details. In the literature, a fine registration via the Iterative Closest Point (ICP) algorithm is usually performed before computing the final C2M analysis (Remondino et al., 2023).

However, the NeRF approach has demonstrated significant advantages in rendering photorealistic textures and handling challenging lighting conditions, delivering high-quality surface details, especially in regions where shadows and reflections complicate the reconstruction. In contrast, SfM algorithms have shown greater computational performance and scalability efficiency, producing accurate geometric reconstructions for areas with clear textures and uniform lighting. Nevertheless, SfM struggles in scenes characterized by non-uniform illumination, strong shadows, specular reflections, or low-light conditions, which can compromise feature detection and matching, ultimately impacting point cloud density and precision (Rabby and Zhang, 2023).

Despite challenges like high computational requirements and the necessity for optimal camera configurations, NeRF shows significant potential in photogrammetry, particularly when high visual fidelity is required. Conversely, SfM is a viable option for projects where geometric accuracy is more critical than photorealism (Müller et al., 2022). These limitations also point to areas of active development: hybrid methods combining the geometric precision of photogrammetry with the photorealistic rendering capabilities of NeRF may represent a future direction for high-fidelity, multi-temporal 3D monitoring applications in complex scenarios (Themistocleous and Abate, 2024).

2. Materials and methods

This paper aims to investigate the possibility of integrating NeRF and photogrammetry to generate images from the same camera poses across different epochs, thereby improving consistency in data over time and making it a valuable tool for multi-temporal analysis. By consistency, we refer to the reduction of variability in image data caused by external factors that typically differ across survey missions. In underwater environments, reproducing identical acquisition conditions over time is particularly challenging. In this study, camera positions and orientations estimated via a photogrammetric approach are later processed by the Nerfacto model of Nerfstudio[1] (Tancik et al., 2023) to generate a virtual reconstruction of the surveyed scene and to create synthesized images (Barron et al., 2022, 2021) from the same point of view across epochs, enabling multi-temporal comparisons (which will be detailed further in the following sections) by analyzing visual data of the same scene acquired at different points in time to identify and quantify changes. The goal is to develop a reliable method for image-based (2D) monitoring of environmental changes, thereby supporting the development of effective conservation strategies. In this study, we do not employ a refraction-aware NeRF specifically tailored for underwater imagery (Zhang and Johnson-Roberson, 2023). Instead, the acquisition setup utilizes a dome port with a central perspective alignment, which minimizes refraction effects and makes them negligible for this work.

2.1 The adopted Photogrammetry-NeRF protocol

In collaboration with marine ecologists, an experiment was conducted on L. stictiforme thalli that were previously fixed to specially designed granite tiles, equipped with four coded photogrammetric targets, to support the metric verification of co-registration between different survey epochs. The data were acquired approximately 38 meters deep in Costa Paradiso, Sardinia, using an Olympus E-M1 Mark II camera with a 9 mm lens and a centered dome port. Additionally, two calibrated scale bars and a 24-patch color checker were included in the surveyed scene to scale the model and perform a radiometric consistency check (for details on the developed acquisition protocol, see Nocerino et al., 2025).

The proposed workflow (Figure 1) relies on generating photorealistic underwater scenes using synthetic rendering techniques. Two monitoring epochs, t_0 and t_1, were acquired under different illumination conditions, camera positions, and acquisition geometries. The two acquisition epochs were intentionally separated in time, introducing natural environmental variability, such as lighting differences, sedimentation, and biological modifications, thereby allowing for the assessment of ecologically plausible changes.

[1] Nerfstudio Version 1.1.5 (https://docs.nerf.studio/)

The study focused on three main aspects: a) correction of radiometry to allow a normalized comparison among the different epochs of the monitoring period; b) generation of the 3D model via a standard photogrammetric approach and a NeRF approach, and check of the metric consistency of the models generated via NeRF approach via a Cloud to Mesh (C2M) comparison; c) generation of novel synthesized image from predefined point-of-view for all the monitoring epochs to help the domain's experts assess the health status of the L. *stictiforme;* d) Assessment of image comparison and analysis to detect visual changes among t_0 and t_1 epoch images.

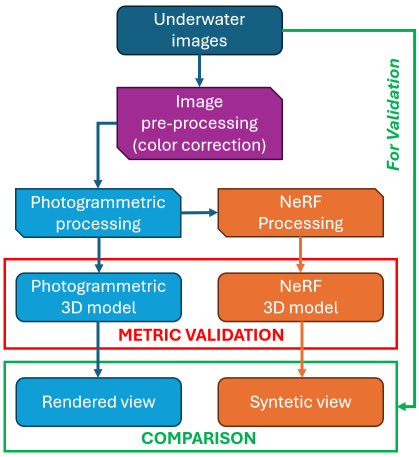

Figure 1. Workflow adopted in this study for generating photorealistic underwater scenes through synthetic rendering techniques.

3. Image pre-processing: Correction of radiometry

Underwater photogrammetry provides highly accurate spatial reconstructions; however, it presents challenges in maintaining radiometric accuracy due to environmental conditions, including light absorption and scattering (Jaffe, 1990). Therefore, the collected images were pre-processed and radiometrically corrected.

In our experiments, we used artificial lighting to mitigate the attenuation of natural light underwater and restore the whole spectrum. However, this results in non-uniform illumination of the acquired images (see the vignetting effect in Figure 2). Most existing underwater color enhancement methods are not designed to work in the presence of artificial lighting (Shuang et al., 2024). In our experience (Calantropio et al., 2024), when red channel attenuation is minimized, as in the case of shallow water acquisition or the use of artificial light, a white balance correction may sufficiently improve the image radiometry Nonetheless, while the validation performed on an underwater color checkerboard (Table 1 and Figures 2, 3, and 4) confirmed the effectiveness of the correction, it does not correctly account for the spatially variable illumination conditions and does not ensure uniform appearance throughout the image set.

All ROIs	Original image (whitebalanced)	Agisoft Metashape Render	Nerfstudio Render
ΔE $\bar{x}$	8,60	15,94	9,67

Table 1. Average color difference (ΔE) across all 24 color patches in the CIELAB space. The values compare the white-balanced image, a photogrammetric render (Metashape), and a NeRF-based render (Nerfstudio) against the reference color checkerboard. Lower ΔE values indicate better color fidelity.

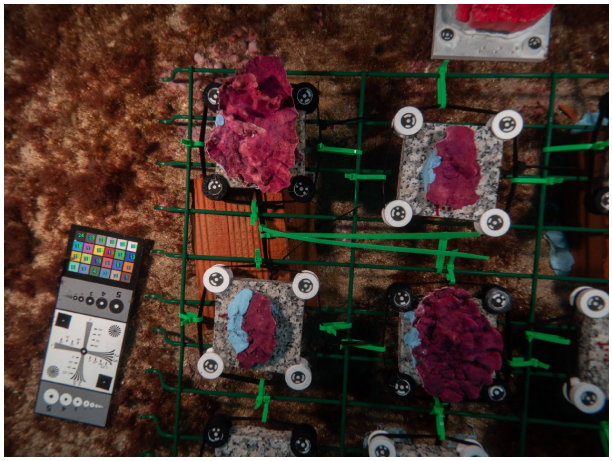

Figure 2. Original (real) underwater image after white balance correction. The colored checkerboard used for radiometric validation is visible in the scene, with specific regions of interest (ROIs) highlighted for color accuracy analysis.

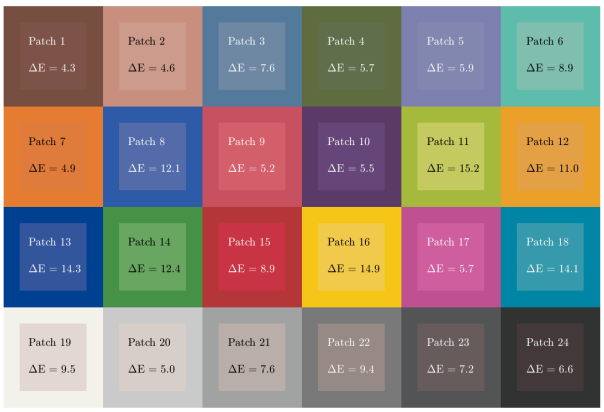

Figure 3. Color accuracy evaluation for the white-balanced image. The filled squares represent the measured colors for each region of interest (ROI), while the thick surrounding borders correspond to the reference colors on the color checkerboard.

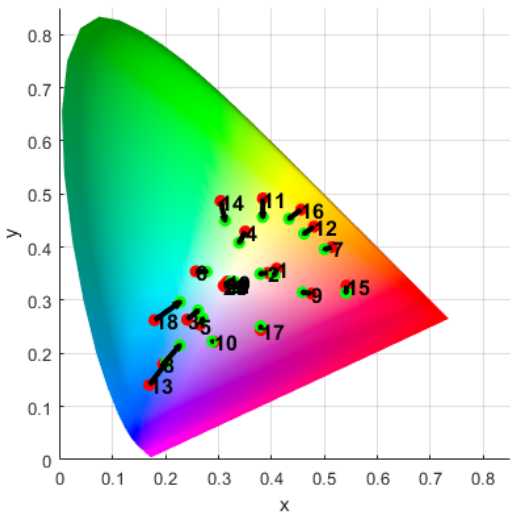

Figure 4. The diagram shows the measured and reference colors in the CIE 1976 L*a*b* color space on a chromaticity diagram. Red circles denote the reference color, while green circles represent the measured color of each color patch. The chromaticity diagram does not convey the brightness of colors, but only their α and β components.

4. Data processing: SfM and NeRF approaches

In this study, photogrammetry was employed to estimate the relative orientation of cameras, while scene scaling was achieved through calibrated scale bars, enabling high-resolution 3D models. A marker-based co-registration approach facilitated the temporal comparison between two epochs (t_0 and t_1), leveraging four coded photogrammetric targets placed on each tile (Nocerino et al., 2025). Due to the high computational demand of the NeRF implementation adopted, training was not conducted on the entire image dataset. Instead, a representative subset of images—covering the same spatial extent—was selected and used consistently for both the NeRF (training at full resolution) and photogrammetric workflows (processing at full resolution) to ensure a fair and controlled comparison. The photogrammetric and NeRF-based processing and evaluation were realized using the hardware configuration detailed in Table 2.

Component	Specification
Operating System	Microsoft Windows 11 Pro, Version 10.0.26100 Build 26100
Processor	Intel(R) Core(TM) i7-14700K, 3.40 GHz, 20 cores / 28 threads
Memory (RAM)	32.0 GB
GPU	NVIDIA GeForce RTX 4080 SUPER

Table 2. Hardware specifications used for processing and analysis performed in this research

To assess the spatial accuracy and consistency of the NeRF-derived reconstructions, the NeRF-derived point cloud was compared (after performing fine registration via the Iterative Closest Point algorithm) with the corresponding mesh generated photogrammetrically using Agisoft Metashape, which served as the ground truth for each epoch (t_0 and t_1). All C2M analyses were performed using CloudCompare[2], and the results are reported in Table 3 and visualized in Figure 5.

C2M distance [mm]	t_0 NeRF	t_1 NeRF
Mean	1.30	0.38
Std. dev	6.37	6.51

Table 3. Cloud-to-Mesh (C2M) distance statistics for each epoch. The mean and standard deviation values (in millimeters) summarize the spatial discrepancies between the dense point clouds and their corresponding 3D meshes for NeRF-derived reconstructions at two time points (t_0 and t_1).

5. Generation of photogrammetry-based renders and NeRF novel synthesized images

In the framework of this research, the synthesized views were created in Nerfstudio using camera interior and exterior orientation parameters derived from photogrammetric Bundle Block Adjustment (BBA).

The synthesized images generated from photogrammetry and NeRF pipelines reproduced the original camera resolution (5184 × 3888 pixels) and Field of View (FoV), enabling a direct pixel-wise comparison. This was achieved through the Nerfacto method within the modular PyTorch framework Nerfstudio, which was configured to avoid downscaling during training (via the command line ns-train NeRFacto -- data-- downscale-factor 1), thereby preserving the original image resolution. While this approach resulted in higher computational demands, the gain in texture and lighting realism was deemed essential, especially for assessing chromatic and morphological changes in ecologically sensitive substrates such as crustose coralline algae (Figure 6).

From a performance standpoint, the trade-off between NeRF's computational cost and visual fidelity appears justified in this context. High-resolution synthetic imagery facilitates quantitative comparisons and qualitative ecological interpretation, supporting expert assessments of substrate condition, degradation, or recovery. Integrating NeRF and SfM may offer a promising hybrid solution: NeRF could enrich visual realism and semantic interpretation, while SfM ensures robust geometric precision. Such a combined approach could significantly improve the multi-temporal monitoring of underwater ecosystems, particularly in applications where structural metrics and perceptual fidelity are crucial.

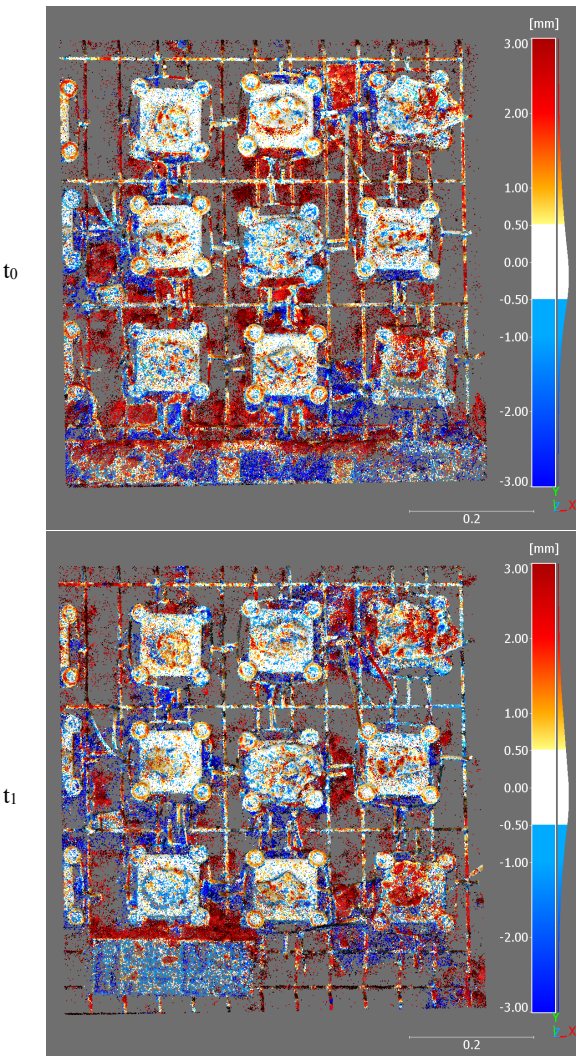

Figure 5. Cloud-to-Mesh (C2M) distance analysis visualizing the geometric discrepancies between the NeRF-derived point cloud and the corresponding photogrammetric mesh for epochs t_0 (top) and t_1 (bottom). The photogrammetric mesh was treated as ground truth.

[2] CloudCompare Version 2.13.2 (https://www.cloudcompare.org/)

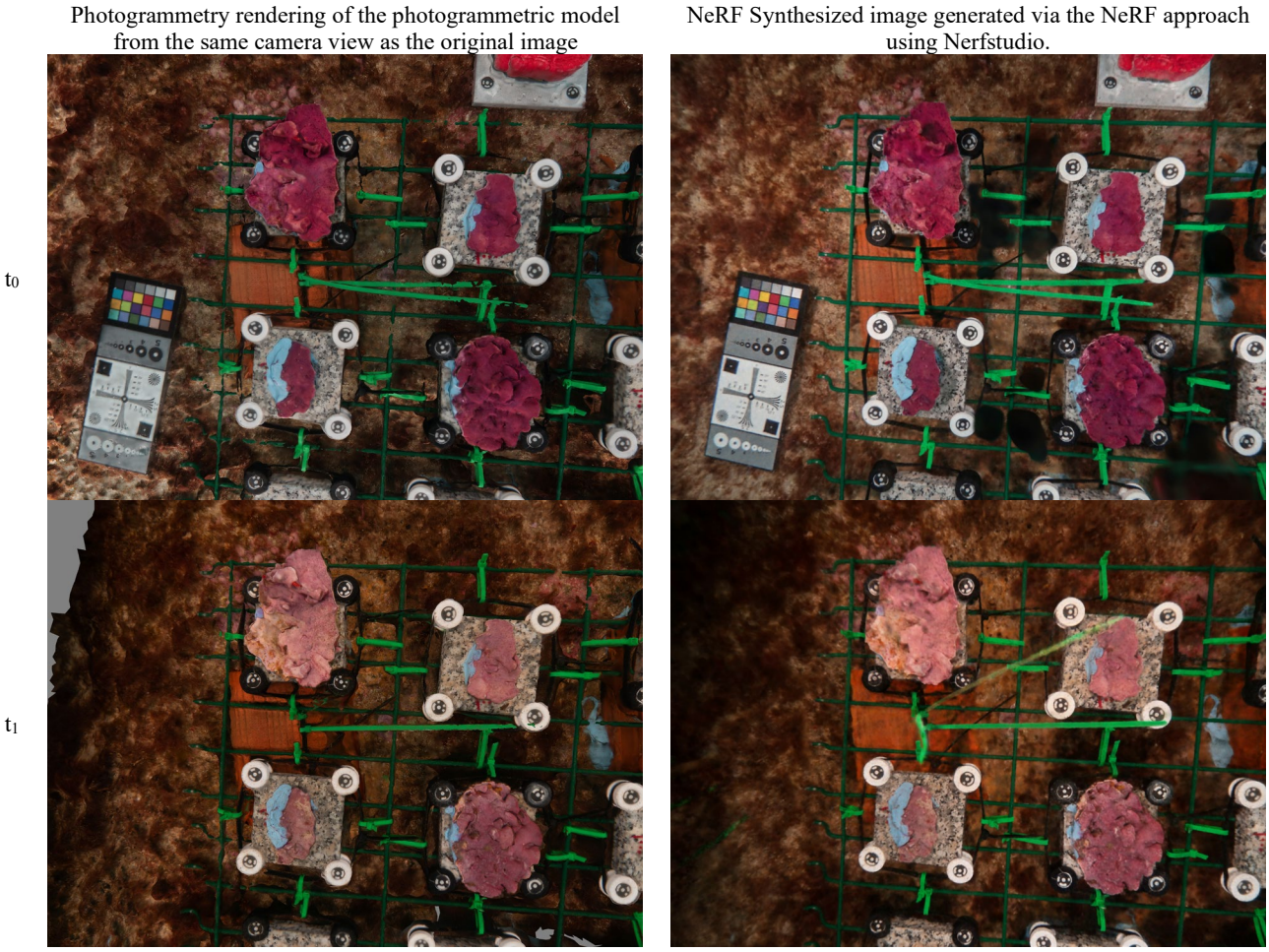

Figure 6. High-resolution synthesized views generated in Metashape (photogrammetry - left) and Nerfstudio (NeRF - right) at epochs t_0 (top) and t_1 (bottom). The images were rendered using camera interior and exterior orientation parameters derived from photogrammetric processing. Each synthesized image matches the original underwater acquisition format (5184 × 3888 pixels) and Field of View (FoV), with no downscaling applied during NeRFacto training. These views enable accurate multi-temporal comparisons under ecologically realistic variability.

6. Image Comparison and Analysis

A spatially consistent binary mask was defined to isolate the region of interest (ROI) where changes would be evaluated across the two time epochs. The same imaging setup was employed to render photogrammetric and NeRF-derived models from identical camera viewpoints, allowing colorimetric comparisons.

Once the synthesized views were generated, several evaluation metrics were applied, including Structural Similarity Index Measure (SSIM), Peak Signal-to-Noise Ratio (PSNR), and color difference (ΔE). SSIM is a perceptual metric that quantifies image quality degradation caused by processing or compression. It compares the structural information (luminance, contrast, and texture) between two images, providing a value between -1 and 1, where 1 indicates perfect similarity. PSNR measures the ratio between the maximum possible signal (image intensity) and the noise introduced by compression or distortion. It is expressed in decibels (dB), with higher values indicating better image quality. It is most effective when comparing images with the exact dimensions and color depth. ΔE quantifies the difference between two colors in a perceptual color space (commonly CIELAB). A ΔE value 0 means no difference, while larger values indicate greater perceptual differences. It is often used in applications requiring precise color reproduction and comparison.

Results showed good visual consistency and structural alignment between the image couples, although some residual differences were observed. These deviations were likely due to radiometric artifacts, limitations inherent in NeRF training, and minor environmental changes between the two acquisition epochs.

A detailed analysis was conducted to quantitatively assess changes between the two temporally separated images of the same underwater scene. This focused on the same ROI identified earlier, with background elements excluded using the predefined binary mask. Phase correlation was employed for image registration, yielding a negligible translation vector and a registration error of only 1.0 pixel. This result confirms subpixel alignment between the images, providing a solid foundation for a subsequent accurate pixel-wise comparison.

Pixel-wise similarity metrics were computed to assess image-level discrepancies. The Mean Squared Error (MSE) indicated a moderate average difference in pixel intensities. The PSNR values, relatively low in both cases, reflected visible differences, particularly in regions with high contrast or variable

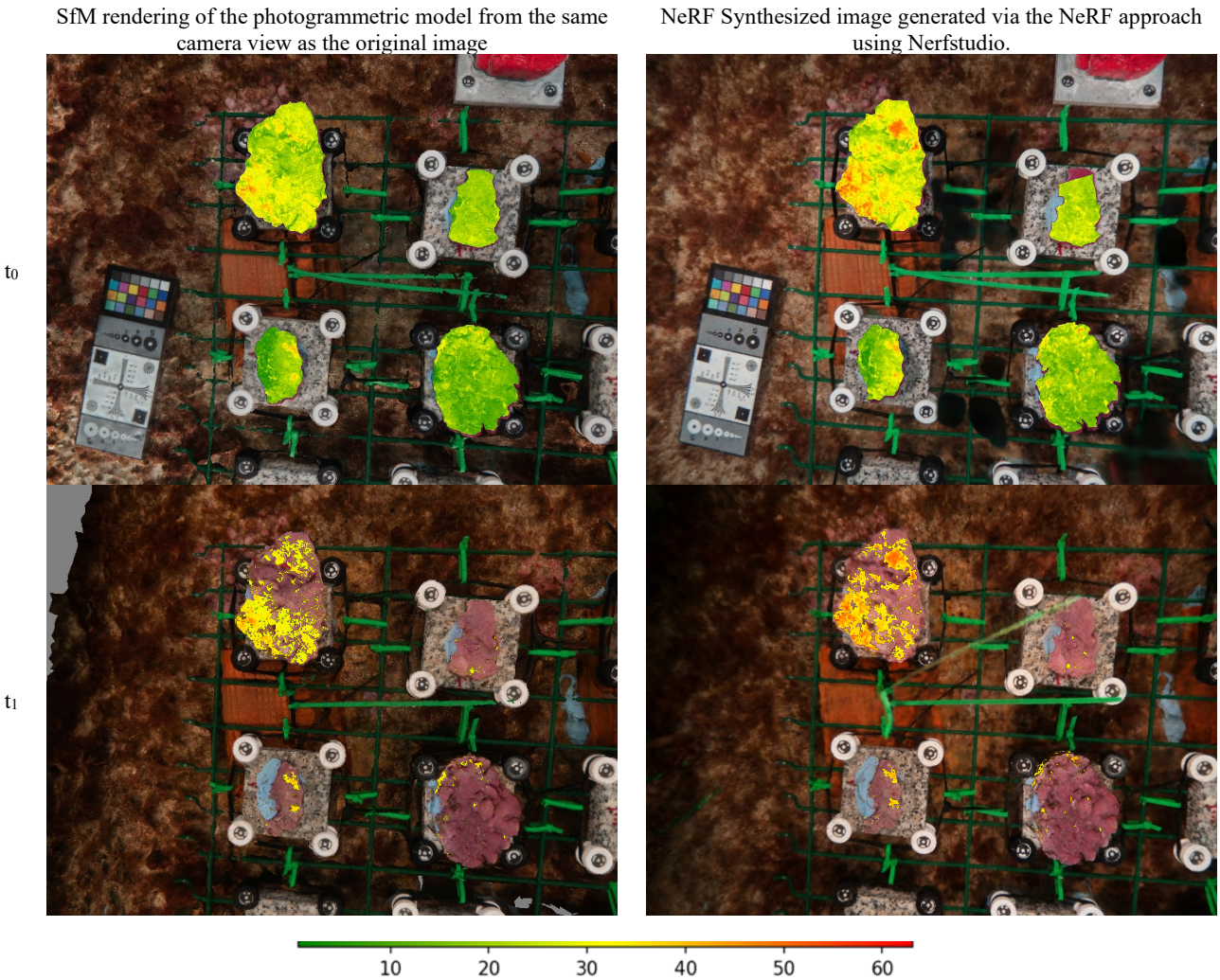

Figure 7. Side-by-Side Comparison Panel that displays the rendered images, both overlays, and the color scale, facilitating direct visual assessment of changes. Full-scene (top) and top-20% (bottom) overlays were produced using a green-to-red colormap, where green indicates minimal perceptual change and red represents the most significant differences. A reference scale bar helps interpret ΔE heatmaps.

lighting. Specifically, values below 20 dB suggest these differences are likely noticeable. The SSIM values demonstrated moderate structural similarity; values below 0.7 imply discernible variation in texture, luminance, or spatial organization.

Chromatic variation was further assessed using the perceptual color difference metric ΔE, computed in the CIELAB color space. Comparisons were made between photogrammetric renderings and NeRF-generated synthesized images for both time points. The ΔE results confirmed that most color changes were perceptible to the human eye, with ΔE values exceeding the threshold of 2.3. High mean and median values pointed to widespread variations potentially driven by environmental factors, material differences, or biological degradation of the observed samples.

A color-coded overlay visualization was employed to support interpretation. The ΔE maps were displayed using a green-to-red colormap, where green indicated minimal perceptual change and red represented substantial deviation. Two visual outputs were created: a full-scene ΔE heatmap showing all differences within the ROI, and a focused overlay highlighting the top 20% of pixels with the most significant changes. A horizontal scale bar was added to guide the interpretation of these overlays and facilitate ecological insight (Figure 7). Quantitative values are summarized in Table 4.

Metric	t_0 vs t_1 render (SfM)	t_0 vs t_1 syntetic images (NeRF)
Registration shift	[0 0.], error: 1.0	[0 0.], error: 1.0
MSE	1.119.342	1.150.454
PSNR	14.82 dB	13.52 dB
SSIM	0.5765	0.6419
ΔE Min	0.00	0.64
ΔE Max	68.94	63.06
ΔE Mean	21.57	24.37
ΔE Median	21.12	23.58

Table 4. Quantitative comparison of synthesized image renderings from photogrammetric (SfM) and NeRF-derived models between time epochs t_0 and t_1 within a predefined Region of Interest (ROI). Metrics include registration shift (in pixels), Mean Squared Error (MSE), Peak Signal-to-Noise Ratio (PSNR), Structural Similarity Index Measure (SSIM), and perceptual color difference (ΔE) in CIELAB space. Results reflect geometric alignment accuracy, structural coherence, and colorimetric variation, with ΔE values indicating widespread perceptible changes likely driven by environmental and radiometric factors.

7. Results and discussion

To improve monitoring accuracy, integrating photogrammetry with NeRF techniques has significant implications for monitoring activities. By generating synthesized images based on 3D models, it is possible to directly compare data from different eras while reducing the influence of external factors by minimizing the variability in image data that arises from non-structural changes (those not related to actual changes in the monitored object or site, but rather to environmental or acquisition conditions) providing, for instance, consistent lighting and viewpoint, effectively removing these sources of inconsistency.

Conservation efforts can be focused on the areas most affected by habitat degradation, allowing timely environmental interventions. Future experimentations will include validating this monitoring protocol to expand its applicability to other domains, such as archaeological excavations, where activities consist of repeated surveys over time to ensure complete site documentation. In the face of growing environmental challenges, advanced monitoring solutions will be crucial to ensuring the long-term conservation and resilience of aquatic ecosystems, playing a key role in the future of marine conservation and ecological monitoring.

8. Conclusions

This study introduces a novel approach to the multi-temporal monitoring of crustose coralline algae (CCA) using synthesized underwater image generation. By assessing real-world environmental changes, we produced ground-truth-validated synthesized views that are a basis for testing photogrammetry AI-boosted monitoring techniques. Applying a comprehensive image comparison framework, which includes structural and colorimetric metrics, provides insights into the temporal changes within CCA-dominated benthic assemblages.

The results demonstrate that significant alterations can be detected over time, with substantial perceptual chromatic differences (as revealed by ΔE metrics). The framework supports the detection of ecological shifts and contributes to the development of automated tools for long-term monitoring of underwater ecosystems. By generating synthesized images from a constant point of view across different epochs, this approach circumvents the limitations associated with real-world image acquisition, such as inconsistencies in camera pose estimation across surveys, which complicates multi-temporal analysis. The ability to render images from fixed, photogrammetrically defined principal points eliminates such discrepancies, ensuring geometrically consistent datasets over time, providing a reproducible and reliable method for ecological monitoring.

Underwater settings inherently limit image quality and coverage due to turbidity, lighting attenuation, and diver-induced variability. While this study successfully adapted NeRF to such constraints, future investigations could benefit from data augmentation strategies or domain adaptation to improve performance under suboptimal acquisition conditions.

In this study, we did not employ a refraction-aware NeRF specifically tailored for underwater imagery (Zhang and Johnson-Roberson, 2023). Instead, the acquisition setup utilized a dome port with a central perspective alignment, which minimizes refraction effects and allows them to be considered negligible for this work. Nevertheless, acknowledging the potential impact of complex refraction in more challenging scenarios, a future research direction will involve testing NeRF-based models explicitly designed to account for refractive geometry. This will enable a more comprehensive evaluation of their benefits and limitations in underwater photogrammetric applications.

Integrating this method into real-time monitoring systems could offer a robust means of assessing ecosystem health and identifying early warning signals for climate-related disturbances. Future work will focus on expanding the applicability of this methodology to more complex and diverse marine environments, as well as enhancing the resolution and realism of synthetic image generation to better address the challenges of real-world underwater image-based monitoring.

Acknowledgment

The authors acknowledge financial support under the National Recovery and Resilience Plan (NRRP), Mission 4, Component 2, Investment 1.1, Call for tender No. 104 published on 2.2.2022 by the Italian Ministry of University and Research (MUR), funded by the European Union – NextGenerationEU– Project Title MANATEE – CUP I53D23001970006- Grant Assignment Decree No. 961 adopted on 30/06/2023 by the Italian Ministry of University and Research (MUR)

References

Barron, J.T., Mildenhall, B., Tancik, M., Hedman, P., Martin-Brualla, R., Srinivasan, P.P., 2021. Mip-NeRF: A Multiscale Representation for Anti-Aliasing Neural Radiance Fields. Presented at the Proceedings of the IEEE/CVF International Conference on Computer Vision, pp. 5855–5864.

Barron, J.T., Mildenhall, B., Verbin, D., Srinivasan, P.P., Hedman, P., 2022. Mip-NeRF 360: Unbounded Anti-Aliased Neural Radiance Fields. Presented at the Proceedings of the IEEE/CVF Conference on Computer Vision and Pattern Recognition, pp. 5470–5479.

Calantropio, A., Chiabrando, F., Menna, F., Nocerino, E., 2024. Quantitative Evaluation of Color Enhancement Methods for Underwater Photogrammetry in Very Shallow Water: a Case Study. ISPRS Ann. Photogramm. Remote Sens. Spat. Inf. Sci. X-2–2024, 25–32. https://doi.org/10.5194/isprs-annals-X-2-2024-25-2024

Croce, V., Billi, D., Caroti, G., Piemonte, A., De Luca, L., Véron, P., 2024. Comparative Assessment of Neural Radiance Fields and Photogrammetry in Digital Heritage: Impact of Varying Image Conditions on 3D Reconstruction. Remote Sens. 16, 301. https://doi.org/10.3390/rs16020301

Jaffe, J.S., 1990. Computer modeling and the design of optimal underwater imaging systems. IEEE J. Ocean. Eng. 15, 101–111. https://doi.org/10.1109/48.50695

Mildenhall, B., Srinivasan, P.P., Ortiz-Cayon, R., Kalantari, N.K., Ramamoorthi, R., Ng, R., Kar, A., 2019. Local Light Field Fusion: Practical View Synthesis with Prescriptive Sampling Guidelines. https://doi.org/10.48550/arXiv.1905.00889

Mildenhall, B., Srinivasan, P.P., Tancik, M., Barron, J.T., Ramamoorthi, R., Ng, R., 2020. NeRF: Representing Scenes as Neural Radiance Fields for View Synthesis. https://doi.org/10.48550/arXiv.2003.08934

Müller, T., Evans, A., Schied, C., Keller, A., 2022. Instant neural graphics primitives with a multiresolution hash encoding. ACM Trans Graph 41, 102:1-102:15. https://doi.org/10.1145/3528223.3530127

Nocerino, E., Del Pizzo, S., Lambertini, A., Troisi, S., Vittuari, L., 2023. MANATEE Project: Monitoring and Mapping of Marine Habitat with Integrated Geomatics Technologies, in: 2023 IEEE International Workshop on Metrology for the Sea; Learning to Measure Sea Health Parameters (MetroSea). Presented at the 2023 IEEE International Workshop on Metrology for the Sea; Learning to Measure Sea Health Parameters (MetroSea), pp. 181–186. https://doi.org/10.1109/MetroSea58055.2023.10317544

Pepe, M., Alfio, V.S., Costantino, D., 2023. Assessment of 3D Model for Photogrammetric Purposes Using AI Tools Based on NeRF Algorithm. Heritage 6, 5719–5731. https://doi.org/10.3390/heritage6080301

Pinna, F., Caragnano, A., Piazzi, L., Ragazzola, F., Stipcich, P., Rindi, F., Ceccherelli, G., 2022. The Mediterranean bioconstructor Lithophyllum stictiforme shows adaptability to future warming. Front. Mar. Sci. 9. https://doi.org/10.3389/fmars.2022.930750

Rabby, A.S.A., Zhang, C., 2023. BeyondPixels: A Comprehensive Review of the Evolution of Neural Radiance Fields. https://doi.org/10.48550/ARXIV.2306.03000

Remondino, F., Karami, A., Yan, Z., Mazzacca, G., Rigon, S., Qin, R., 2023. A Critical Analysis of NeRF-Based 3D Reconstruction. Remote Sens. 15, 3585. https://doi.org/10.3390/rs15143585

Shuang, X., Zhang, J., Tian, Y., 2024. Algorithms for improving the quality of underwater optical images: A comprehensive review. Signal Process. 219, 109408. https://doi.org/10.1016/j.sigpro.2024.109408

Tancik, M., Weber, E., Ng, E., Li, R., Yi, B., Kerr, J., Wang, T., Kristoffersen, A., Austin, J., Salahi, K., Ahuja, A., McAllister, D., Kanazawa, A., 2023. Nerfstudio: A Modular Framework for Neural Radiance Field Development, in: ACM SIGGRAPH 2023 Conference Proceedings, SIGGRAPH '23.

Themistocleous, K., Abate, D., 2024. Photogrammetry and NeRF techniques are used to document built heritage, in: Earth Resources and Environmental Remote Sensing/GIS Applications XV. Presented at the Earth Resources and Environmental Remote Sensing/GIS Applications XV, SPIE, pp. 272–277. https://doi.org/10.1117/12.3031605

Zhang, T., Johnson-Roberson, M., 2023. Beyond nerf underwater: Learning neural reflectance fields for accurate color correction of marine imagery. IEEE Robot. Autom. Lett. 8, 6467–6474.